NASA/TM–2013-218142

Remote Sensing of Dissolved Oxygen and Nitrogen in Water Using Raman Spectroscopy

Rene Ganoe
Science Systems and Applications, Inc., Hampton, Virginia

Russell J. DeYoung
Langley Research Center, Hampton, Virginia

December 2013

NASA STI Program . . . in Profile

Since its founding, NASA has been dedicated to the advancement of aeronautics and space science. The NASA scientific and technical information (STI) program plays a key part in helping NASA maintain this important role.

The NASA STI program operates under the auspices of the Agency Chief Information Officer. It collects, organizes, provides for archiving, and disseminates NASA's STI. The NASA STI program provides access to the NASA Aeronautics and Space Database and its public interface, the NASA Technical Report Server, thus providing one of the largest collections of aeronautical and space science STI in the world. Results are published in both non-NASA channels and by NASA in the NASA STI Report Series, which includes the following report types:

- TECHNICAL PUBLICATION. Reports of completed research or a major significant phase of research that present the results of NASA Programs and include extensive data or theoretical analysis. Includes compilations of significant scientific and technical data and information deemed to be of continuing reference value. NASA counterpart of peer-reviewed formal professional papers, but having less stringent limitations on manuscript length and extent of graphic presentations.

- TECHNICAL MEMORANDUM. Scientific and technical findings that are preliminary or of specialized interest, e.g., quick release reports, working papers, and bibliographies that contain minimal annotation. Does not contain extensive analysis.

- CONTRACTOR REPORT. Scientific and technical findings by NASA-sponsored contractors and grantees.

- CONFERENCE PUBLICATION. Collected papers from scientific and technical conferences, symposia, seminars, or other meetings sponsored or co-sponsored by NASA.

- SPECIAL PUBLICATION. Scientific, technical, or historical information from NASA programs, projects, and missions, often concerned with subjects having substantial public interest.

- TECHNICAL TRANSLATION. English-language translations of foreign scientific and technical material pertinent to NASA's mission.

Specialized services also include organizing and publishing research results, distributing specialized research announcements and feeds, providing information desk and personal search support, and enabling data exchange services.

For more information about the NASA STI program, see the following:

- Access the NASA STI program home page at *http://www.sti.nasa.gov*

- E-mail your question to help@sti.nasa.gov

- Fax your question to the NASA STI Information Desk at 443-757-5803

- Phone the NASA STI Information Desk at 443-757-5802

- Write to:
  STI Information Desk
  NASA Center for AeroSpace Information
  7115 Standard Drive
  Hanover, MD 21076-1320

NASA/TM–2013-218142

Remote Sensing of Dissolved Oxygen and Nitrogen in Water Using Raman Spectroscopy

Rene Ganoe
Science Systems and Applications, Inc., Hampton, Virginia

Russell J. DeYoung
Langley Research Center, Hampton, Virginia

National Aeronautics and
Space Administration

Langley Research Center
Hampton, Virginia 23681-2199

December 2013

Available from:

NASA Center for AeroSpace Information
7115 Standard Drive
Hanover, MD 21076-1320
443-757-5802

Abstract

The health of an estuarine ecosystem is largely driven by the abundance of dissolved oxygen and nitrogen available for maintenance of plant and animal life. An investigation was conducted to quantify the concentration of dissolved molecular oxygen and nitrogen in water by means of Raman spectroscopy. This technique is proposed for the remote sensing of dissolved oxygen in the Chesapeake Bay, which will be utilized by aircraft in order to survey large areas in real-time. A proof of principle system has been developed and the specifications are being optimized to maximize efficiency for the final application. The theoretical criteria of the research, components of the experimental system, and key findings are presented in this report.

I. Introduction

Dissolved oxygen (DO), i.e. molecular oxygen (O_2), in ocean waters is critical for stability and survival of marine ecosystems and organisms. Declining DO concentrations will elicit dire consequences for global biogeochemical cycles, marine habitats, and the native organisms. Diminished concentrations of DO can be fatal, and for most aquatic species this critical point is ~4 mg/L DO in water [1]. Areas of water with oxygen concentrations under 2 mg/L are hypoxic and considered anoxic once concentrations reach 0 mg/L. Anoxic areas are referred to as dead zones, which are primarily located in coastal waters due to shallow water depth, abundance of biological activity, and tangency to land [2]. Currently, less than 25% of dead zones have DO measurements, so there is a need for more efficient methods of mapping concentrations in large-scale coastal areas [3].

A substantial portion of the Chesapeake Bay, the largest estuary in the United States, is considered critically hypoxic or anoxic. The use of fertilizer for crop production, resulting in a large input of reactive nitrogen compounds and phosphorous through direct deposition by wastewater run-off and atmospheric deposition, is the primary contributor to coastal hypoxia in the Chesapeake Bay [4]. The increased discharges add a surplus of nutrients, a process known as eutrophication. Hypoxia due to eutrophication occurs when an overabundance of nutrients in the water enable rapid increase of algae populations, known as algal blooms. The algae in these blooms are short lived, and microbes readily decompose the remaining organic material. This process of microbial degradation generates an aberrant increase in aerobic respiration activity, causing the microbes to rapidly consume oxygen; thus, depleting the DO content of the water [5]. A recent scientific overview states that coastal eutrophication has become an increasingly urgent global concern that is responsible for the steady growth in the magnitude and persistence of hypoxic coastal waters [6].

The current measurement technique for dissolved oxygen is Optode technology, which requires direct in-situ measurements. An optode is an optical sensor device that uses a chemical transducer to measure a specific substance [7]. Optodes are spatially limited, as they require direct contact with the water. The extended time it requires a vessel to travel the entirety of the measurment region allows variation in water conditions to occur and produces readings that are not temporally aligned [8]. A national interagency scientific assessment committee agree on the insufficiency of current ship-based surveys due to the temporal dynamics of hypoxia; nonetheless, advocate that this can be resolved through “new technologies for measuring dissolved oxygen, that can be deployed in the field to provide continuous measurements” [9].

Water in coastal regions continuously comes in contact with air due to low depth and active currents; therefore, the predominant gases dissolved in ocean water are molecular nitrogen (N_2) and oxygen (O_2). Studies have shown that sea water is virtually saturated with dissolved nitrogen and therefore the concentration remains constant regardless of biological activity [10]. Despite oxygen being more water soluble than nitrogen, its concentration is lower due to overall higher abundance of atmospheric nitrogen. The relative volume percent concentration of N_2 in sea water is 63.3% compared to 35.6% for O_2, assuming 100% saturation of both gases at 1 atm (up to depth of approx. 10m) [11]. A discrepancy in the N_2 to O_2 ratio (1.78) would indicate the extent of DO depletion; thus, it is necessary to measure both O_2 and N_2 to fully evaluate the concentration of dissolved gases.

This paper will describe a new Raman remote sensing technique that could measure the concentration of DO and N_2 from aircraft throughout the Chesapeake Bay or other water body. This remote sensing technique will allow high resolution, real-time measurement of critically important dissolved gases; furthermore, these measurements could substantially improve our understanding of the temporal and spatial dynamics of dissolved gas distributions in maritime coastal ecosystems. The goal of this research effort is to provide evidence that remote sensing of water using Raman spectroscopy is a viable approach to measure both O_2 and N_2 in coastal waters; and subsequently, provide groundwork to design an aircraft based lidar system for spatial and temporal mapping of O_2 and N_2 in coastal regions such as the Chesapeake Bay.

II. Experimental Setup

In the remote DO Raman sensing technique, a pulsed UV laser is directed into a water specimen. The UV laser emission induces an electric dipole moment, thus changing the molecular polarizability and bringing the O_2 and N_2 molecules to a virtual excited state. The difference in energy between the ground and virtual states create a wavelength shift, radiating longer wavelength Raman emission at a wavelength specific to the polarization potential characteristic of the molecule [12]. This shifted emission wavelength is backscattered to the lidar receiver where it is detected. The detected signal is directly proportional to the water concentration of O_2 and N_2 [13]. The Raman differential scattering cross-section (cm^2/sr), which is needed to quantify the probability of photon-molecule interaction, varies inversely with the fourth power of the excitation laser wavelength [12]. The Raman shifts for 355nm laser excitation, corresponding wavelengths, and cross sections of molecular species pertinent to this work are shown in Table 1.

Table 1. Raman shifts, corresponding wavelengths, and scattering cross sections of relevant backscatter molecules

Molecular Species	Raman shift (cm^{-1})	λ (nm)	σ, 10^{-30} cm^2/sr [14, 15]
O_2	1556	376.2	1.1
H-O-H (bending mode, ν_2)	1640	377.4	0.54
N_2	2331	387.5	2.1
O-H (symmetric stretch, ν_1)	3450	405.1	56.3

A schematic of the experimental setup appears in Figure 1. A flashlamp pumped Nd-YAG Laser (Continuum PL9050), is Q-switch operated at a repetition rate of 30Hz, with a power of

1.8 W at 355nm. The YAG fundamental pulse output is frequency tripled using a KTP nonlinear crystal and generates a pulse at the third harmonic; these parameters are outlined in Table 2.

Table 2. Third Harmonic Generation Performance Parameters

Energy	60 mJ
Stability	±4%
Pulsewidth	7ns
Polarization	>95% horizontal
Linewidth	$1.5cm^{-1}$
Repetition Rate	30 Hz

The third harmonic provides the excitation wavelength of 355nm. Near UV excitation wavelengths are optimal for Raman scattering from O_2 and N_2, which provide relatively weak signals particularly in liquid medium. The intensity of Raman scattering decreases as the fourth power of the wavelength, so using shorter laser excitation wavelengths are preferred [12].

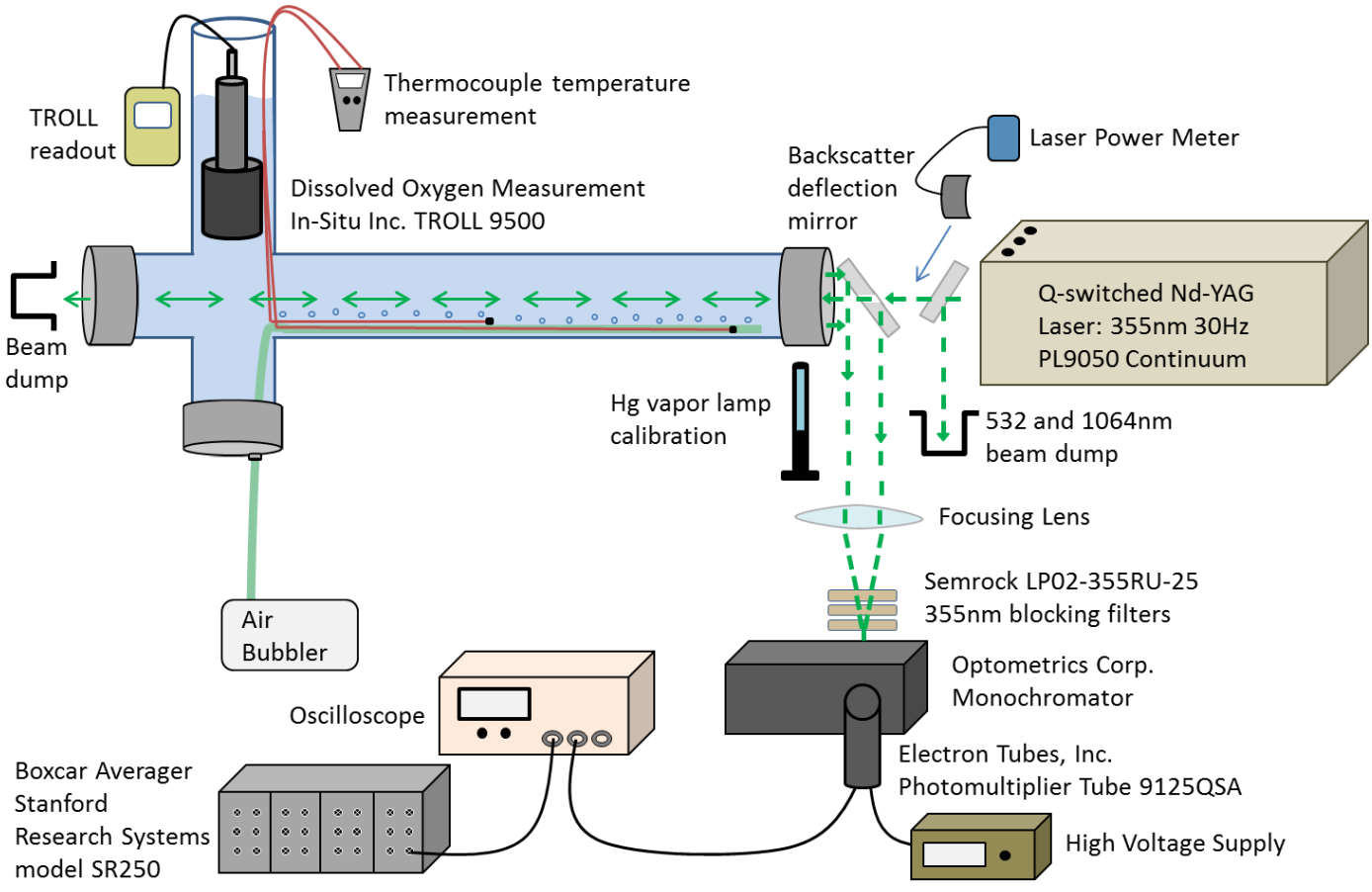

Figure 1. Raman scattering dissolved oxygen/nitrogen experimental setup.

The 355nm pulses pass through a hole in a 10cm diameter flat aluminum coated deflection mirror and into a 1.88m x 10cm diameter glass water cell. As the beam passes through the water

cell, the UV photons excite molecules in the beam path, producing inelastic Raman scattering. The backscattered photons pass back through the water cell and are deflected off the aluminum flat mirror to the focusing lens, which directs the light into a monochromator (Optometrics Corp., model SDMC1-01). The monochromator transmits only the manually selected wavelength of UV light, and is fitted with 355nm blocking filters (Semrock # LPO2-355RU-25) to attenuate the noise signal received from the 355nm laser. A photomultiplier tube (PMT) (Electron Tubes, Inc., 9125QSA) on the monochromator converts the photons into an electrical signal that can be detected by an oscilloscope. In conjunction with the oscilloscope, a gated integrator and boxcar averager module (Stanford Research Systems SR250) acquires and analyzes the PMT signals, increasing the signal to noise ratio by averaging.

The water cell has an attached vertical column to house a Troll 9500 dissolved oxygen in situ monitor (In-Situ Inc Troll 9500). The Troll measures an array of water parameters, such as: temperature, barometric pressure, conductivity, pH, and dissolved oxygen. Troll measurements are used for calibration of DO concentration measurements in the experimental setup. The specifications of these sensors are provided in Table 3. To attain maximum solubility of the dissolved gases in the glass cell during tests, an air bubbler is utilized to saturate the water. Bubbler tubes run up through the water cell's vertical portion and are fitted along the bottom of the horizontal tube. A thermocouple temperature measurement records water temperature and two thermocouple wires are fitted to the bubbler tubes that run the length of the water cell. The outer perimeter of the glass cell is wrapped with heating tapes to facilitate increasing the water temperature.

Table 3. Troll 9500 Sensor Specifications

Conductivity Type:4-cell conductivity, AC drive Operating range: Low: 5µS/cm 20,000µS/cm High:150µS/cm to 112,000µS/cm Accuracy: Low: ±0.5% or 2µS/cm High:±0.5% +2µS/cm Resolution: Range-dependent Pressure rating: 350 psi (246m, 807ft) Operating temperature: 5°C to 50°C	Temperature Type: Platinum resistance thermometer Range: -5°C to 50°C Accuracy: ±0.1°C Resolution: 0.01°C Barometric pressure Type: Piezoresistive Si pressure sensor Range: 0-16.5 psia (854mm Hg, 33.6in Hg) Accuracy: ±0.3% FS (2.54mm Hg,0.1in Hg) Resolution: 0.1mm Hg, 0.01in Hg
Dissolved oxygen Type: Optical, fluorescence quenching Range: 0 to 20 mg/L, 0 to 450% saturation Pressure rating: 300 psi Operating temperature: 0°C to 40°C Accuracy: ±0.1 mg/L @ 0-8 mg/L ±0.2 mg/L @ 8-20 mg/L Resolution: 0.01 mg/L	pH Type: Glass sensing bulb, single junction electrode, replaceable ceramic junction, refillable reference electrolyte Range: 0 to 12 pH units Pressure rating: 350 psi (246m, 807ft) Operating temperature: 0°C to 50°C Accuracy: ±0.1 pH unit Resolution: 0.01 pH unit

For calibration of the Troll measurement, distilled water was air bubbled and DO content was measured as a function of time to determine the rate of water saturation. After approximately 20 minutes of bubbling, the water reaches full DO saturation, as shown in Figure 2. Upon full saturation, the DO content was measured as a function of gradually increasing water temperature in order to confirm an accurate solubility measurement of DO. The solubility attained by the Troll measurement is congruent with the literature value [16], as shown in Figure 3.

Water temperature recordings are an average of measurements from three locations along the water cell, and are maintained within 0.5°C. The Troll 9500 measurement utilizes automatic internal salinity correction factors, which adjust the recorded conductivity (µS/cm or PSU) of the water. Theoretical DO content (mg/L) at 100% saturation must be manually corrected by salinity factors, which are given by the conductivity at various water temperatures [16].
The sample of water used for testing was retrieved from the Back Bay, VA, a tributary of the Chesapeake Bay near NASA Langley Research Center, Hampton, VA.

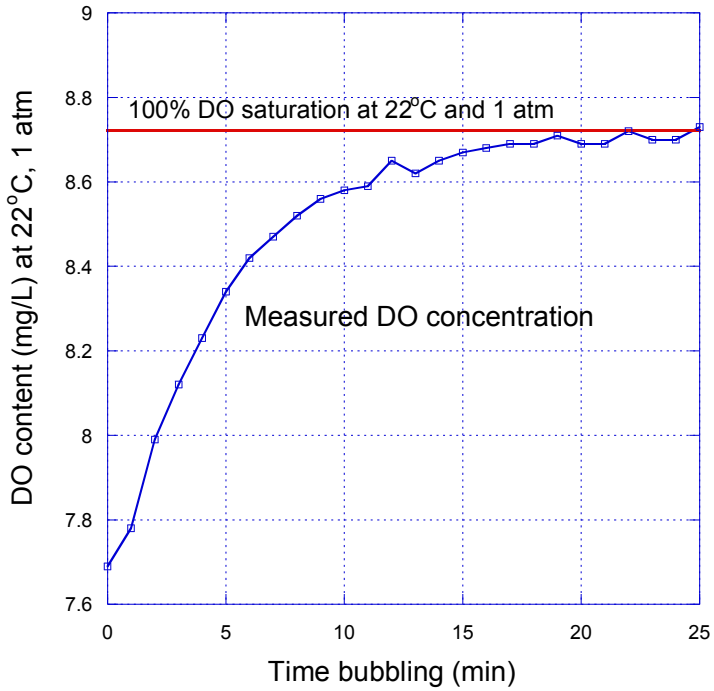

Figure 2. Saturation time of DO (mg/L) in water at 22°C, 1 atm.

Due to the experimental configuration, a gap between the deflection mirror and water cell creates an air interface. The possibility that this interface is the source of the detected oxygen and nitrogen signals was eliminated when the water cell window was blocked, and all signal intensity immediately dropped to noise; thus, the detected bands are a product of inelastic Raman backscattering within the water cell.

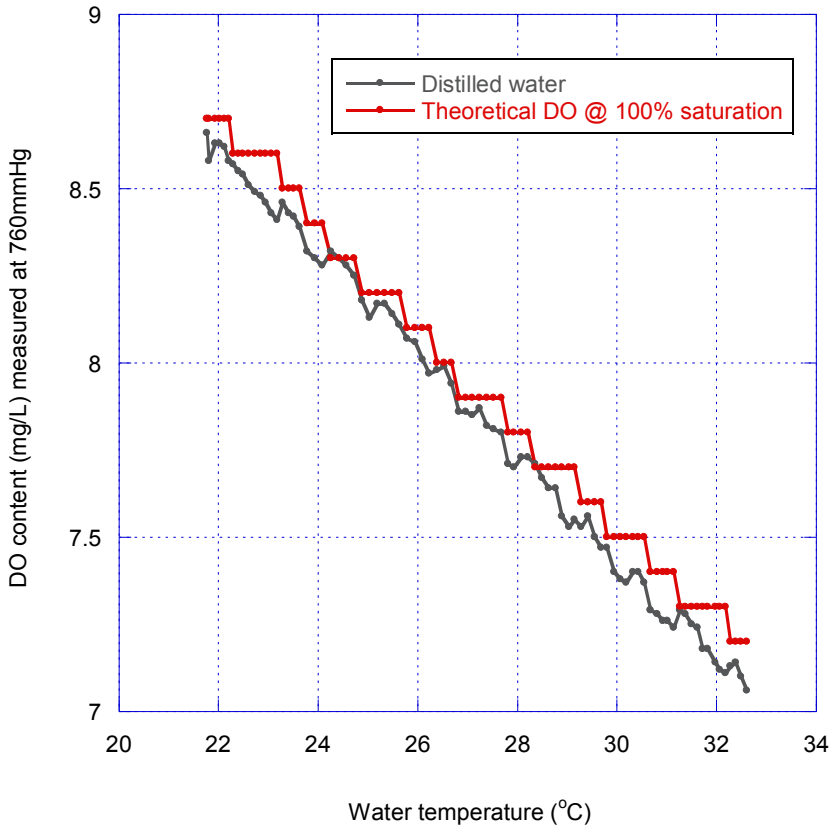

.

Figure 3. Experimentally acquired by the Troll solubility of DO (mg/L) in distilled water with increasing water temperature compared with theoretical prediction given by tabulated values [16].

III. Dynamics of Dissolved Gases in Water

A study by Emerson et al [17] quantitatively measured the total gas pressure in water to exist as it does in the atmosphere, thus as the sum of its partial pressures of constituent gases. To obtain the total gas pressure in water (w) in terms of N_2 and O_2 in water, it must be assumed that Ar, H_2O, and CO_2 are at equilibrium with the atmosphere (a), hence,

$$p^{\mathrm{w}}_{\mathrm{Ar}} + p^{\mathrm{w}}_{\mathrm{H_2O}} + p^{\mathrm{w}}_{\mathrm{CO_2}} = p^{\mathrm{a}}_{\mathrm{Ar}} + p^{\mathrm{a}}_{\mathrm{H_2O}} + p^{\mathrm{a}}_{\mathrm{CO_2}} \quad (1)$$

These species often have large variablilities in sea water, but are present at such miniscule concentrations that this assumption does not affect measurement accuracy by more than 0.2%. The partial pressure of the dissolved gas is related to its concentration in seawater, as a function of temperature and salinity. This function creates the solubility coefficient, the reciprocal of which is equivalent to the Bunsen coefficient [17].

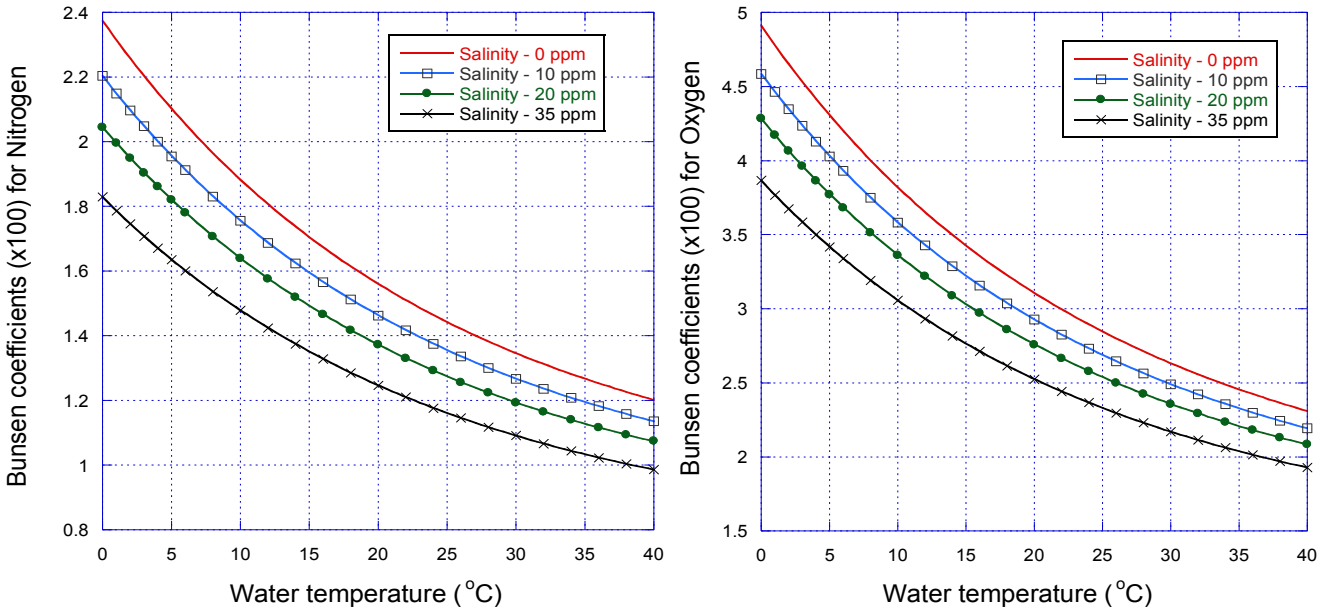

Figure 4a & b. Bunsen coefficients for N_2 (a) and O_2 (b) vs water temperature as function of salinity concentration [18].

The Bunsen coefficient (B_G) is used to describe gas solubilities in liquids, and is defined as the volume of a gas absorbed per unit volume liquid at a specific temperature of measurement, when the partial pressure of that gas is 1atm [19]. Any unit of volume can be used to describe the gas and liquid volumes, as long as both are the same [20]. The Bunsen coefficient is dependent on salinity as well as temperature, as shown in Figures 4a & b. This coefficient describes the solubility of a dissolved gas as a unitless value [21].

The gas partial pressure in water is the gas pressure that would be in equilibrium with the seawater concentration at the measured temperature and salinity. At saturation equilibrium, the partial pressure of gases in surface water are equal to the values in a water vapor saturated atmosphere [17]. As water depth increases, the absolute pressure increases and thus the partial pressures of the dissolved species increase as well, as shown in Figure 5.

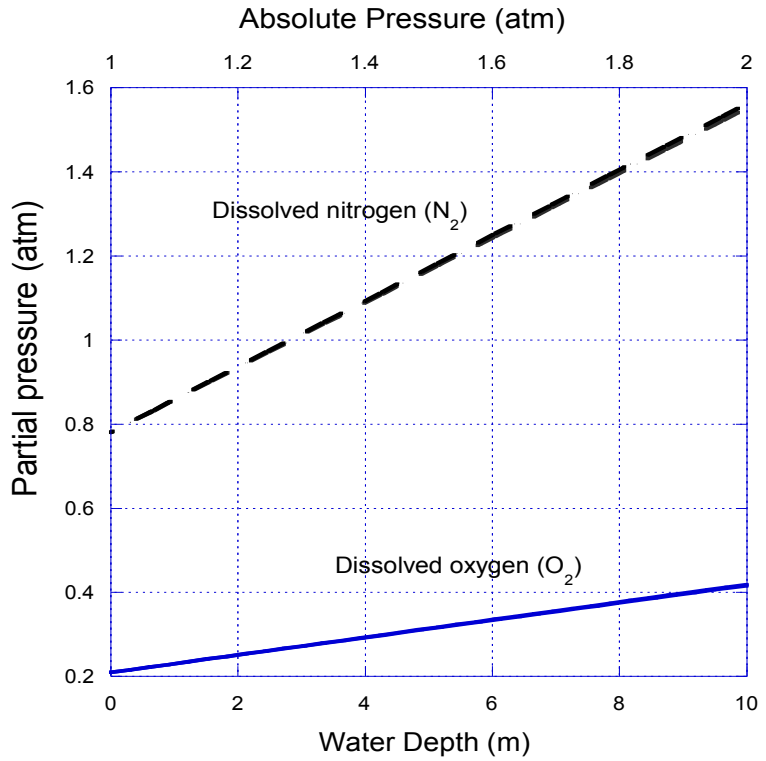

Figure 5. The partial pressures of N_2 and O_2 as functions of water depth and absolute pressure, calculated using the species mole fractions listed in Table 4. At zero water depth the partial pressures are equivalent to the atmospheric partial pressures.

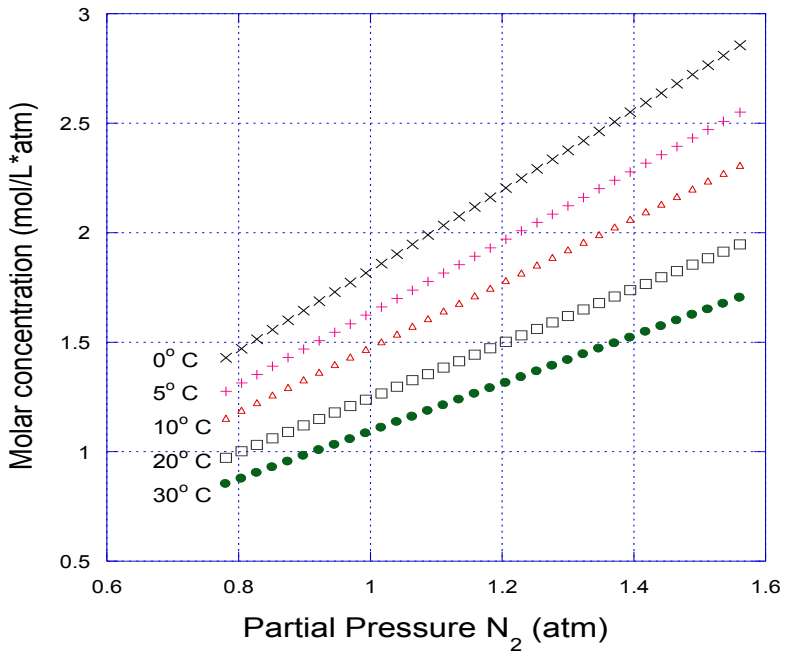

Figure 6. The theoretical concentration of N_2 vs partial pressure per unit air pressure of N_2 as function of water temperature, calculated using equation 2 and the Bunsen coefficients from Figure 4.

Using the Bunsen coefficient to account for the solubility specific to each gas, in conjunction with partial pressure derived by depth, the theoretical concentration of the gas at 100% saturation can be determined, as shown in Figure 6 [19]. This relationship is described by equation 2 as

$$C_{N_2} = P_{N_2} \cdot B_{N_2} \quad (2)$$

where C is the concentration, P is the partial pressure, and B is the Bunsen coefficient; each specific to N_2, but can similarly be applied to O_2. Water temperature, salinity, and depth are all measurable by remote sensing techniques, and an algorithm can be written to account for these variables in real time.

IV. Methodology for Raman Spectroscopic Analysis

For data analysis, all Raman signals are normalized to 1W, 355nm laser power. Wavelength calibration was performed using a Hg vapor lamp. Known Hg wavelengths at 365.19, 366.59 and 404.60 nm were used to calibrate the monochromator [23]. A secondary calibration was performed using the relative position of the 377.4nm Raman water bending mode peak, shown in Figure 7.

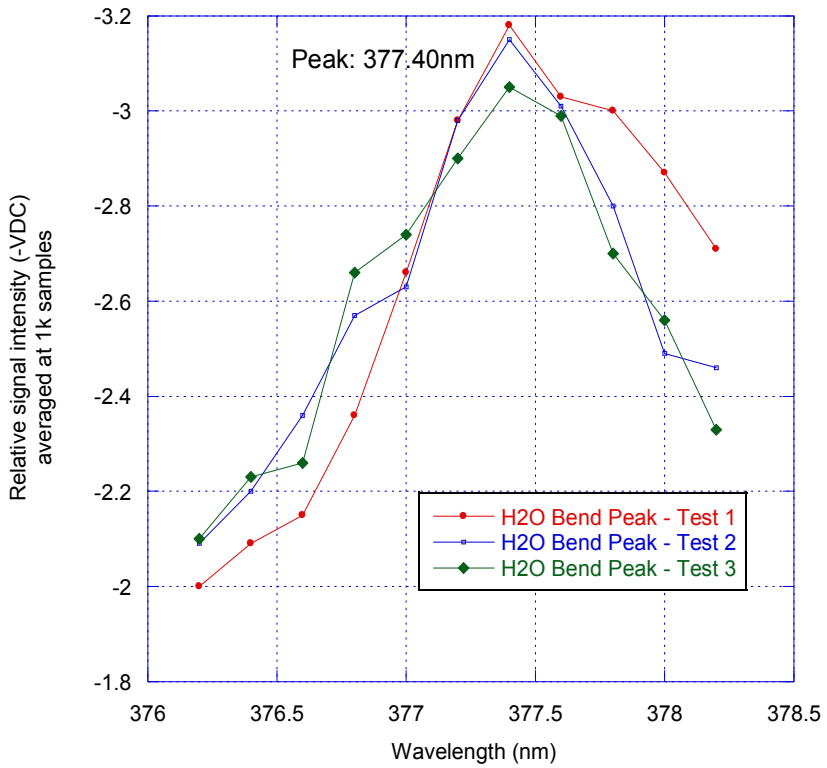

Figure 7. Experimentally acquired monochromator calibration using peak of water bending mode (literature value: 377.40nm) [24].

In order to determine the 355nm laser attenuation through the water medium, the transmittance (*T*) of 355nm light was measured. Theoretical and experimental absorption of distilled water was calculated using equations 3 and 4 respectively. The optical absorption coefficient at 355nm is $0.01517m^{-1}$ for distilled water [25]. Experimental transmission values are taken as a mean of multiple measurements. Total cell window loss was measured and found to be 0.155 absorption.

$I = I_o\, e^{-[0.01517m^{-1} \cdot 1.88m]} = 0.972$ transmittance theoretical (3)
1-0.972 = 0.028 absorption theoretical

$T = I / I_o = 0.78$ transmittance + 0.155 cell window absorption = 0.935 (4)
1-0.930 = 0.065 absorption measured

The measured absorption of distilled water was calculated to be 0.065, which is comparable to the theoretical absorption of 0.028. The discrepancy seen here is likely due to particle accumulation in the water cell over time, increasing sources of scattering. Theoretical and measured absorption of Back Bay water was then calculated using equations 5 and 6 respectively. The optical absorption coefficient at 355nm wavelength is $0.58m^{-1}$ for Back Bay water [26].

$I = I_o\, e^{-[0.58m^{-1} \cdot 1.88m]} = 0.336$ transmittance theoretical (5)
1-0.336 = 0.66 absorption theoretical

$T = I / I_o = 0.0048$ transmittance + 0.155 cell window absorption = 0.1598 (6)
1-0.1598 = 0.84 absorption measured

The measured absorption of Back Bay water was calculated to be 0.84, which is comparable to the theoretical absorption of 0.66. Back Bay water contains an abundance of ionic compounds and organic particulates not found in distilled water, which provide greater scattering of incident light, thus increasing absorption.

Number densities (*n*) of target species, e.g. DO, provide the number of molecules per volume and is used in conjunction with the Raman scattering cross section to determine concentrations of O_2 and N_2 molecules in water. The number density is proportional to the Raman scattering. Number densities were calculated based on the molecular species mass density (ρ) at 100% saturation, 20°C and 1 atm pressure, as shown in equation 7. Avogadro's constant (N_{Av}) refers to the number of molecules in 1 mole of a particular substance, with a value of 6.02214×10^{23} mol^{-1}. The molar mass (M) of that particular substance is determined by the species molecular mass and amount present, expressed in g/mol [27].

$$n = \frac{N_{Av}}{M}\rho \quad (7)$$

The saturation number density calculation for O_2 in seawater accounts for salinity at 35ppt, which lowers maximum saturation; therefore, causing a decrease in mass density from 9.08×10^{-9} kg/cm^3 to 7.2×10^{-9} kg/cm^3. Number density values are provided in Table 4.

Table 4. Properties of pertinent molecular species†

Species†	Number density (n)	Mole fraction[22]
N_2^a	2.19×10^{19} cm^{-3}	0.7808
N_2^w	3.32×10^{17} cm^{-3}	0.6317
O_2^a	5.47×10^{18} cm^{-3}	0.2095
O_2^w	1.71×10^{17} cm^{-3}	0.3359

† (a) is in atmosphere (w) is in water at 1 atm, at 100% saturation

The primary mechanism for quantitative analysis of Raman spectroscopy is the proportional relationship between gas concentration and Raman backscatter intensity [13]. The molecular species concentration can be derived from the Raman scattering intensity and other parameters, as shown by,

$$C = \frac{I_r}{(I_L \, \sigma \, \eta)} \, P \tag{8}$$

where C is the species number density, I_r is the measured Raman backscatter intensity integrated over the band width, I_L is the laser intensity, σ is the species Raman cross-section, η includes instrument parameters (e.g. optical transmission), and P is the sample path length [28]. Variable path length modulates Raman intensity; therefore, peak heights and areas are not necessarily the same for different measurement water depth. In a typical aircraft lidar scenerio the water path length would vary widely and this variance must be accounted for in calculations. Additionally, relative concentrations are independent of path length, and can be determined using the peak ratio method described by Wopenka and Pasteris [29], and specifically employing the two-component system described by Sum et al. [30],

$$\frac{C_{H_2O}}{C_{O_2}} = \frac{A_{H_2O}}{A_{O_2}} \frac{\sigma_{O_2}}{\sigma_{H_2O}} \frac{\eta_{O_2}}{\eta_{H_2O}} \tag{9}$$

where C is the concentration of molecular species in a sample; A is the measured Raman band area, η is the instrument efficiency correction factors and σ is the absolute Raman scattering cross section values. These factors provide a relative, empirically derived, and instrument specific calibration; therefore, must be calculated for each experimental setup [29]. This concentration ratio technique provides an expression comparable to the Beer-Lambert Law and can be applied similiarly, also by creation of a calibration curve. Through Raman measurement, it has been shown that simple gas mixtures yield a linear calibration curve [31].

V. Results and Discussion

Oxygen and nitrogen Raman peaks were initially optimzed in air to confirm wavelengths of the molecular species at 376.2 and 387.55nm, respectively [12]. Raman signals obtained using

the experimental setup were recorded every 0.2nm and scanned between 364.4nm-390.4nm, as shown in Figure 8.

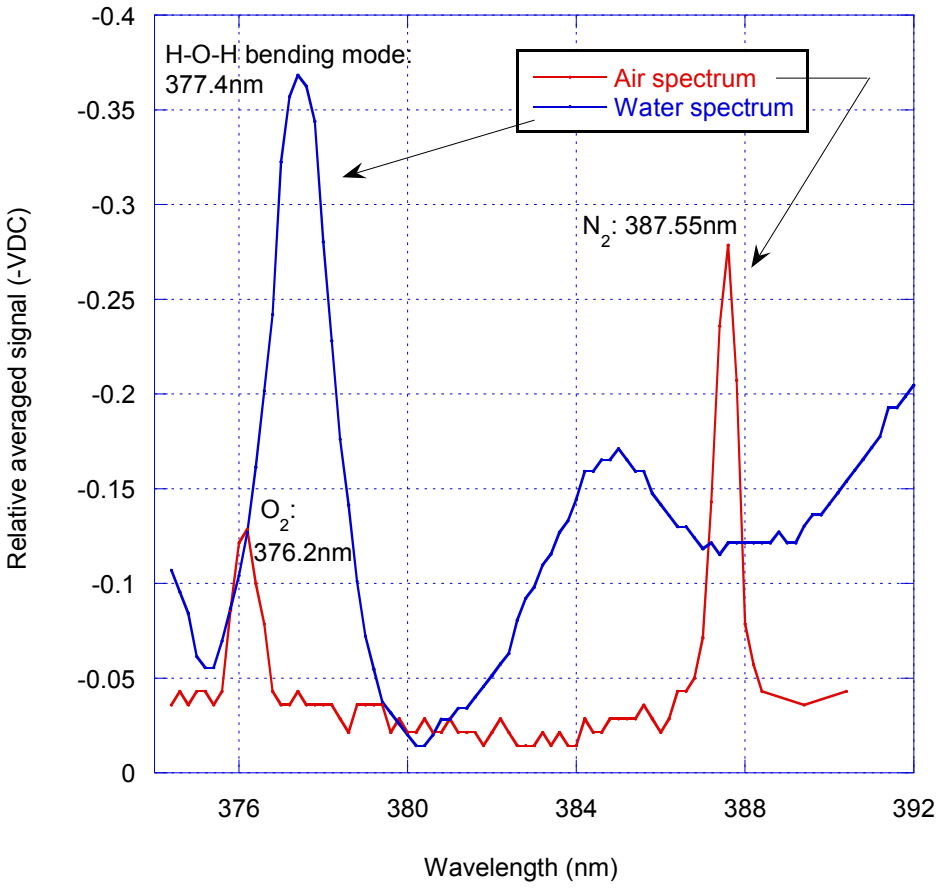

Figure 8. Experimentally measured Raman backscattered spectra of air and water.

A comparison of the N_2 and O_2 number densities noted in Table 4 show that the ratio N_2^a/N_2^w is 66, and O_2^a/O_2^w is 32, thus the Raman scattering intensities are 66 and 32 times below that of the air measurement shown in Figure 8. This significant difference in magnitude is the reason N_2 and O_2 are not visible in the experimentally acquired Raman water spectrum shown in Figure 8.

Due to the inherently lower concentrations of gases in water than that in air, optimizing the O_2 and N_2 backscattered signals require scanning much shorter wavelength increments, 0.02nm, and as an average of 1k samples, increasing signal to noise ratio and thus providing more precise band measurement.

In accordance with solubility laws, the concentration of a gas decreases with increasing water temperature; likewise, in accordance with Raman spectroscopy theory, the concentration of a molecular species is directly proportional to the signal intensity. As the water temperature increases, the signal intensity decreases; thus the N_2 concentration is also decreasing, as shown in the experimental measurements in Figure 9. This data supports that N_2 was in fact observed by

Raman backscattering at 387.55nm. To further justify this outcome, N_2 and O_2 Raman bands were scanned at various levels of DO saturation, as shown in Figures 10 and 11.

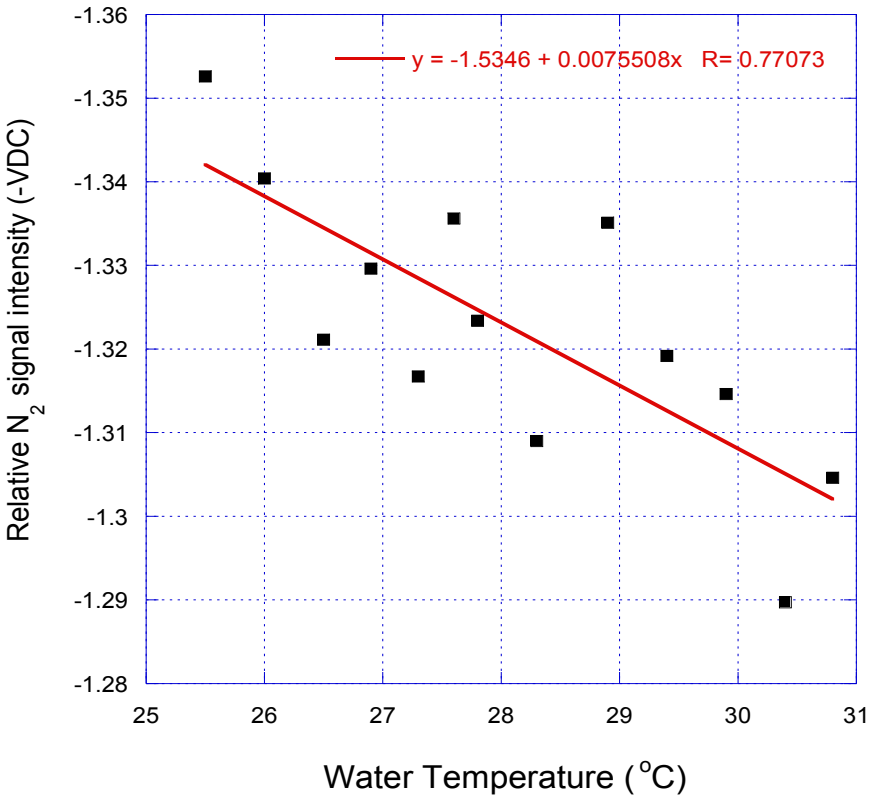

Figure 9. Measured relative N_2 peak intensity at 387.55nm as a function of increasing water temperature.

The Raman N_2 peak band was scanned at two different concentrations of DO; 6.01 and 8.70 mg/L, as shown in Figure 10. The temperature and pressure are the same for both spectra; 24°C and 760 mmHg. Likwise, Figure 11 shows the Raman O_2 peak band scanned at three different concentrations of DO; 6.04, 8.80, and 9.11 mg/L. The temperature and pressure are the same for all three spectra; 24°C and 760 mmHg. The change in peak intensities shown in Figure 11 result from the change in dissolved oxygen content in the water. In this setup, the percent saturation of O_2 can be used to infer the percent saturation of N_2, since there is no biological activity affecting oxygen content, and bubble action produces nearly equal supersaturation for all dissolved gases, as noted in a study by Memery and Merlivat [32]. The concentration of N_2 can then be calculated by the degree of saturation. In seawater, O_2 is produced biologically, so the percent saturation can not be assumed equivocal with N_2, which is an inert gas not affected by biological activity.

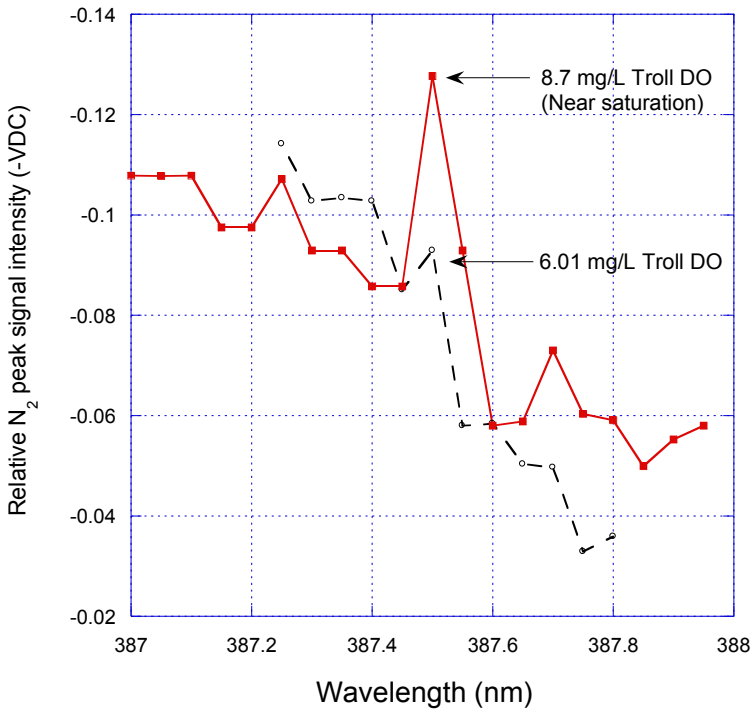

Figure 10. Measured relative intensity of N_2 band peak as function of Troll DO content (mg/L) at 24°C and 1 atm.

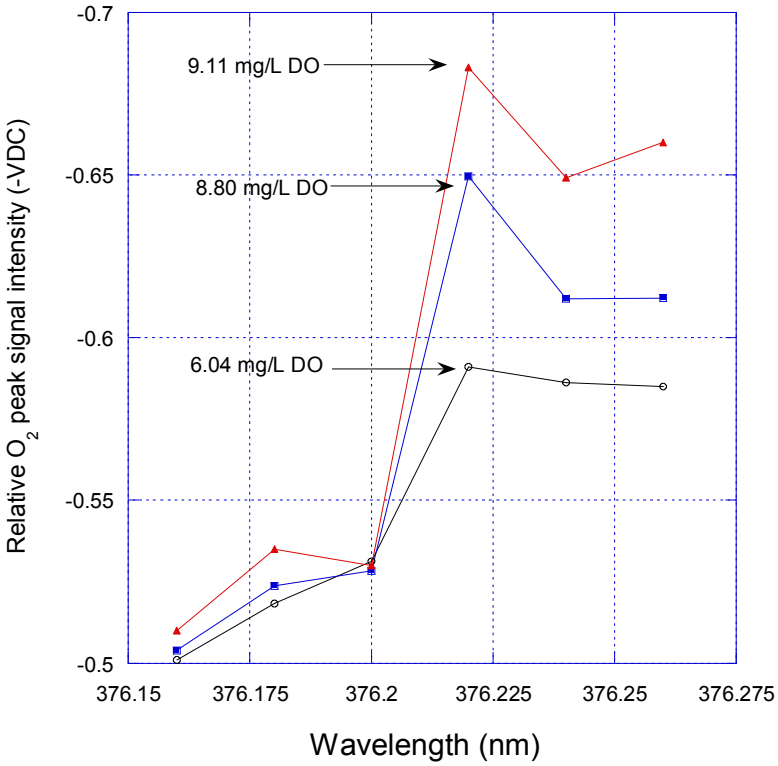

Figure 11. Measured relative intensity of O_2 band peak as function of Troll DO content (mg/L) at 24°C and 1 atm.

Raman spectra can be analyzed by superposition of overlapping bands of non-equivalent species, such as O_2 and the H_2O bending mode. Observation of changes in band width or shape result from a change in the non-equivalent species relative concentrations [13]. Previous researchers have employed comparing Raman water bands with gas species in aqueous phase by use of a ratio technique. A study by White [31] describes utilizing the water stretching band to create a calibration curve which serves as a reference for quantitative analysis. Using this approach, dissolved gas species can be identified and quantified at various pressures, temperatures, and salinity due to the relative constant intensity of the H_2O band. The H_2O peak area, unlike dissolved gas peak areas, does not change in response to variation of those parameters [31].

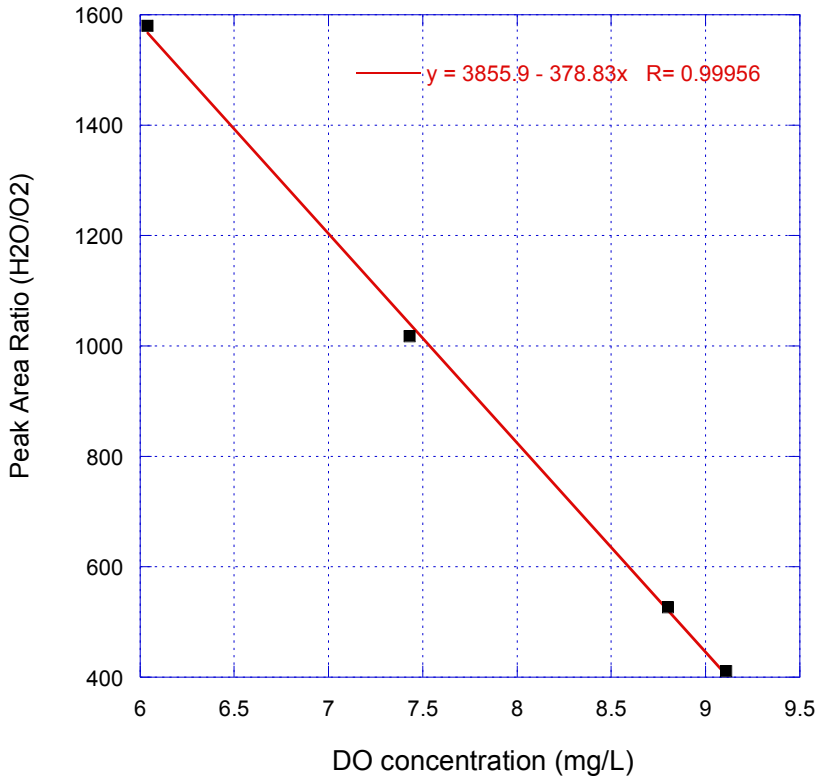

Figure 12. Measured dissolved O_2 concentration as given by Troll vs. H_2O/O_2 peak area ratio in Back Bay water.

Using the Raman experimental setup, a measurement was taken of DO content in Back Bay water, as shown in Figure 12. The area of the O_2 peak at 376.2nm is ratioed to the H_2O bending peak at 377.4nm. The Raman peak areas were calculated using half widths and peak heights measured from the spectrums shown in Figures 7 and 11. The H_2O band area remains constant as a function of DO, so changes in the H_2O/O_2 ratio are attributed to changing O_2 peak area. The Raman peak area of DO is directly proportional to changes in DO concentration. The peak area ratio as a function of DO concentration give a linear calibration curve, which can be used as a quantitative measurement of DO concentration.

With sufficient data, this ratio technique could be used to assemble a calibration curve to show the linear relationship between N_2/O_2 mole fraction ratio and N_2/O_2 Raman peak area

ratios. The mole fraction ratio of a gas mixture directly correlates to the Raman peak area ratio of that gas mixture at the same total pressure. A proportionality constant between the two ratios would provide a linear correlation to convey the level of saturation of the dissolved gases in the water.

The area of a Raman peak of a particular species is quantified as a function of the absolute concentration of the species, Raman cross section of the species, irradiance, and the solid angle of light collection. The absolute concentration is the number of molecules in the scattering volume. The scattering volume, irradiance and solid angle are presumably equivalent for all species simultaneously analyzed in the water column [13]. Therefore, to accurately determine the N_2/O_2 concentration ratio the two species must be scanned over a continous spectrum.

VI. Future Work

The block diagram in Figure 13 illustrates one proposed configuration for the remote Raman sensing flight experiment to measure dissolved gases in coastal waters. The deployment configuration employs the technique described in this paper with the modifications necessary for in flight measurement of dissolved gases in coastal waters.

In order to develop a system capable of acquiring reliable and precise measurements, certain variables must be simultaneously measured, such as water temperature and gas saturation. While DO concentrations (mg/L) can be derived by Raman spectroscopy, the conditions at which those concentrations are measured are also necessary to ensure precision of that measurement. Water temperature can also be measured by Raman spectroscopy, from the change in peak width and intensity of the water bending and stretching modes [33]. Saturation is dependent upon multiple variables itself, such as salinity, and gas exchange across the air-water interface. For calm conditions, the gas exchange constant for oxygen has been shown to increase as the square of the wind velocity, and the exchange flux is proportional to the partial pressure difference between water and air [34,35]. Bubble action, on average, drives ocean water to super-saturation of a few percent for gases such as oxygen. When water is turbulent, this increased bubble exchange can increase the gas exchange constant to a third or fourth power of the wind velocity, as well as alter the proportionality of the exchange flux [34]. The solubility of O_2 and N_2 in water decreases with increased salinity; therefore, salinity adjustments are a necessary component to calculate accurate dissolved gas saturation. Salinity distributions throughout the Chesapeake Bay and its tributaries vary with current, seasonal changes and on a yearly basis [36]. This distribution is commonly mapped by use of airborne microwave radiometry as well as satellite ocean color radiometry [37].

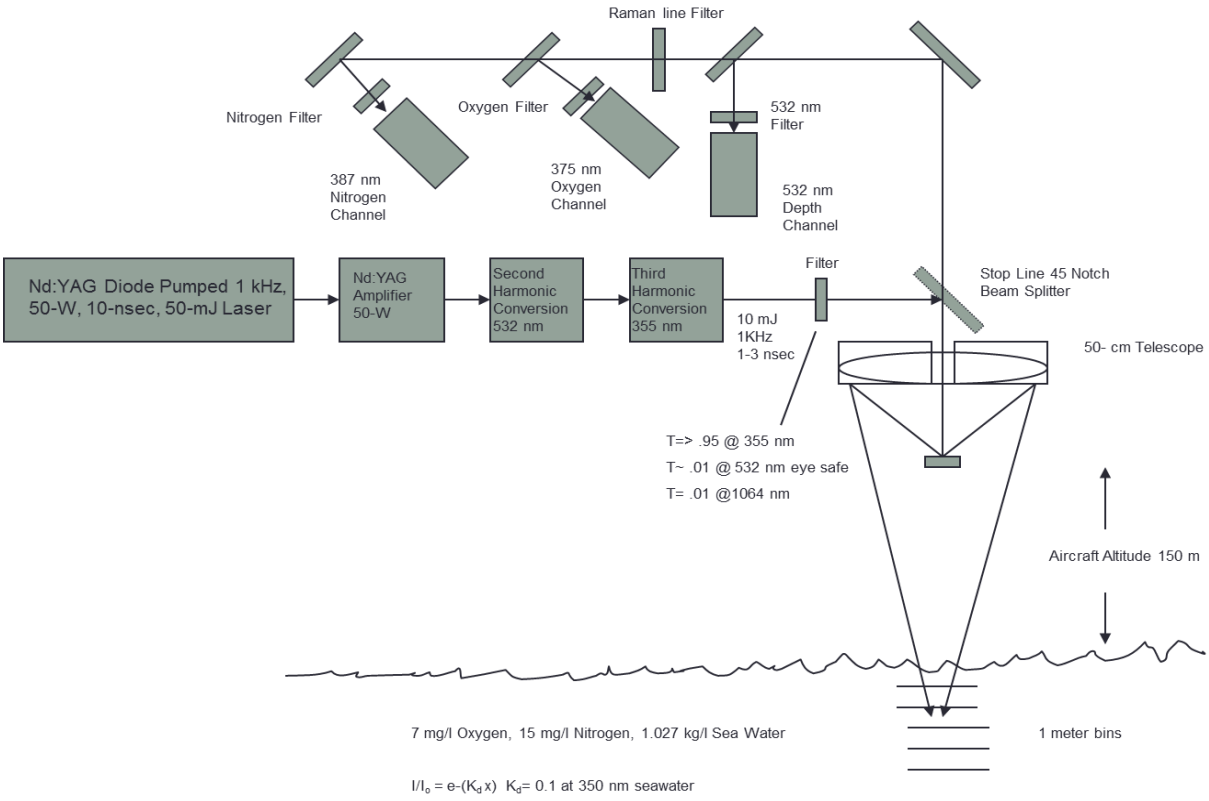

Figure 13. Remote Raman sensing of Oxygen and Nitrogen in coastal waters flight experiment.

VII. Conclusion

A laser system capable of detecting dissolved O_2 and N_2 in water has been demonstrated and is ready for implementation to a remote sensing lidar application. This initial research has been sufficient to demonstrate the theoretical principle, proving the validity of the DO measurement Raman technique. Raman spectroscopic measurement of O_2 and N_2 in water have been performed and shown to produce quantitative measurements when ratioed to the H_2O bending peak. This research represents a novel approach to addressing the problems of hypoxia in estuarine systems, and has shown that it is possible to measure concentrations of dissolved oxygen and nitrogen by a remote sensing technique and has the potential capability to parallel the high accuracy of in-situ DO measurements. This new remote sensing technique will allow much higher temporal and spatial DO measurements at comparable accuracies when compared to current in-situ techniques.

Acknowledgement

The authors wish to acknowledge funding support of Jack Kaye NASA Headquaters, Research and Analysis Program Director.

Reference

[1] Howarth, R., Chan, F., Conley, D.J., Garnier, J., Doney, S.C., Marino, R., Billen, G. Coupled biogeochemical cycles: eutrophication and hypoxia in temperate estuaries and coastal marine ecosystems. Frontiers in Ecology and the Environment 9,1: 18-26, 2011.
[2] Dybas, Cheryl Lyn. "Dead zones spreading in world oceans." *BioScience* 55.7 (2005): 552-557.
[3] Diaz, R.J., Rosenberg, R., Spreading dead zones and consequences for marine ecosystems, Science, 321, 926-929, 2008.
[4] Scavia, D., and M.A. Evans. July hypoxia forecast. University of Michigan. 2012. Testa, J., Winter-spring hypoxia. University of Maryland Center for Environmental Science-Horn Point Laboratory. 2012. http://ian.umces.edu/ecocheck/summer-review/chesapeakebay/2012/indicators/hypoxia/
[5] Diaz, Robert J., and Denise L. Breitburg. "The hypoxic environment." *Fish physiology* 27 (2009): 1-23.
[6] Sutton M.A., et al. (2013) *Our Nutrient World: The challenge to produce more food and energy with less pollution.* Global Overview of Nutrient Management. Centre for Ecology and Hydrology, Edinburgh on behalf of the Global Partnership on Nutrient Management and the International Nitrogen Initiative.
[7] Lubbers, Dietrich W., and Norbert Opitz. "Method and arrangement for measuring the concentration of gases." U.S. Patent No. RE31,879. 7 May 1985.
[8] Tengberg, A., Hovdenes, J., Barranger, D., Brocandel, O., Diaz, R., Sarkkula, J., Huber, C., Stangelmayer, A. Optodes to measure oxygen in the aquatic environment. Sea Technology, 2003.
[9] Committee on Environmental and Natural Resources. 2010. Scientific Assessment of Hypoxia in U.S. Coastal Waters. Interagency Working Group on Harmful Algal Blooms, Hypoxia, and Human Health of the Joint Subcommittee on Ocean Science and Technology. Washington, DC.
[10] The Oceans, Their Physics, Chemistry, and General Biology. New York: Prentice-Hall, 1942.
[11] NASA. 2006. Earth's living ocean: 'the unseen world.' An advanced plan for NASA's ocean biology and biogeochemistry research.
[12] Pelletier, M.J., Quantitative analysis using Raman spectrometry. Applied Spectroscopy 57,1: 20A-42A, 2003.
[13] Hahn, D.W., Raman Scattering Theory, 2007. Department of Mechanical and Aerospace Engineering University of Florida.
[14] Burris, J., McGee, T.J., Heaps, W. UV Raman cross sections in nitrogen. Applied Spectroscopy, 46, 6:1076, 1992.
[15] Xiong, K., Asher, S.A., Lowest energy transition in aqueous Cl- salts: charge transfer transition, The Journal of Physical Chemistry 115: 9345-9348, 2011.
[16] Radtke, D.B., White, A.F., Davis, J.V., Wilde, F.D. Dissolved oxygen. 1998. US Geological Survey, book 9: 27-38.
[17] Emerson, S., Stump, C., Johnson, B., Karl, D.M., In situ determination of oxygen and nitrogen dynamics in the upper ocean. Deep Sea Research I 49: 941-952, 2002.

[18] Weiss, R. F. "The solubility of nitrogen, oxygen and argon in water and seawater." *Deep Sea Research and Oceanographic Abstracts*. Vol. 17. No. 4. Elsevier, 1970.
[19] Weiss, R_F. "Carbon dioxide in water and seawater: the solubility of a non-ideal gas." *Marine chemistry* 2.3 (1974): 203-215.
[20] Wiesenburg, Denis A., and Norman L. Guinasso Jr. "Equilibrium solubilities of methane, carbon monoxide, and hydrogen in water and sea water." *Journal of Chemical and Engineering Data* 24.4 (1979): 356-360.
[21] Craig, H., and R. F. Weiss. "Dissolved gas saturation anomalies and excess helium in the ocean." *Earth and Planetary Science Letters* 10.3 (1971): 289-296.
[22] Glueckauf, E., The composition of atmospheric air, Compendium of Meteorology, American Meteorological Society, Boston, 3-11, 1951.
[23] Sansonetti, C.J., Salit, M.L., Reader, J., Wavelengths of spectral lines in mercury pencil lamps. Applied Optics 35, 1: 74-77, 1996.
[24] Becucci, M., Cavalieri, S., Eramo, R., Fini, L., Materazzi, M., Raman spectroscopy for water temperature sensing, Laser Physics, 9: 1, 422-425, 1999.
[25] Measuring Optical Absorption Coefficient of Pure Water in UV Using the Integrating Cavity Absorption Meter. (May 2008)A Dissertation LING WANG Texas A&M University May 2008
[26] Chesapeake Bay submerged aquatic vegetation water quality and habitat-based requirements and restoration targets: a second technical synthesis. Chapter 4, Factors contributing to water-column light attenuation. Washington: United States Environmental Protection Agency; 2000 Aug.
[27] Mohr, P. J., Taylor, B.N., Newell, D.B. CODATA Recommended values of the fundamental physical constants. Reviews of Modern Physics, 80 (2): 633–730.
[28] White, S.N., Qualitative and quantitative analysis of CO2 and CH4 dissolved in water and seawater using laser Raman spectroscopy, Applied Spectroscopy 64, 7: 819-827, 2010.
[29] Wopenka, B., Pasteris, J.D., Raman intensities and detection limits of geochemically relevant gas mixtures for a lser Raman microprobe. Analytical Chemistry 59: 2165-2170, 1987.
[30] Sum, A.K., Burruss, R.C., Sloan, E.D., Measurement of clathrate hydrates via Raman spectroscopy. Journal of Physical Chemistry 101: 7371-7377, 1997.
[31] White, S.N., Brewer, P.G., Peltzer, E.T., Determination of gas bubble fractionation rates in the deep ocean by laser Raman spectroscopy. Marine Chemistry 99: 12-23, 2006.
[32] Merlivat, L., Memery, L., Gas exchange across an air– water interface: Experimental results and modeling of bubble contribution to transfer. Journal of Geophysical Research 88, 707–724: 1983.
[33] Leonard, D. A., B. Caputo, and F. E. Hoge. "Remote sensing of subsurface water temperature by Raman scattering." *Applied Optics* 18.11 (1979): 1732-1745.
[34] Keeling, R.F., On the role of large bubbles in air-sea gas exchange and supersaturation in the ocean. Journal of Marine Research 51, 2: 237-271, 1993.
[35] Liss, P.S., Processes of gas exchange across an air-water interface. Deep-Sea Research 20: 221-238, 1973.
[36] Williams, M., Longstaff, B., Buchanan, C., Llanso, R., Dennison, W., Development and evaluation of a spatially-explicit index of Chesapeake Bay health, Marine Pollution Bulletin, 59: 14-25, 2009.
[37] Klemas, V., Remote sensing techniques for studying coastal ecosystems: an overview. Journal of Coastal Research 27,1: 2-17, 2011.

REPORT DOCUMENTATION PAGE

Form Approved
OMB No. 0704-0188

1. REPORT DATE *(DD-MM-YYYY)*	2. REPORT TYPE	3. DATES COVERED *(From - To)*
01- 12 - 2013	Technical Memorandum	

4. TITLE AND SUBTITLE

Remote Sensing of Dissolved Oxygen and Nitrogen in Water Using Raman Spectroscopy

5a. CONTRACT NUMBER

5b. GRANT NUMBER

5c. PROGRAM ELEMENT NUMBER

6. AUTHOR(S)

Ganoe, Rene; DeYoung, Russell J.

5d. PROJECT NUMBER

5e. TASK NUMBER

5f. WORK UNIT NUMBER

509496.02.08.05.07

7. PERFORMING ORGANIZATION NAME(S) AND ADDRESS(ES)

NASA Langley Research Center
Hampton, VA 23681-2199

8. PERFORMING ORGANIZATION REPORT NUMBER

L-20259

9. SPONSORING/MONITORING AGENCY NAME(S) AND ADDRESS(ES)

National Aeronautics and Space Administration
Washington, DC 20546-0001

10. SPONSOR/MONITOR'S ACRONYM(S)

NASA

11. SPONSOR/MONITOR'S REPORT NUMBER(S)

NASA/TM-2013-218142

12. DISTRIBUTION/AVAILABILITY STATEMENT

Unclassified - Unlimited
Subject Category 43
Availability: NASA CASI (443) 757-5802

13. SUPPLEMENTARY NOTES

14. ABSTRACT

The health of an estuarine ecosystem is largely driven by the abundance of dissolved oxygen and nitrogen available for maintenance of plant and animal life. An investigation was conducted to quantify the concentration of dissolved molecular oxygen and nitrogen in water by means of Raman spectroscopy. This technique is proposed for the remote sensing of dissolved oxygen in the Chesapeake Bay, which will be utilized by aircraft in order to survey large areas in real-time. A proof of principle system has been developed and the specifications are being honed to maximize efficiency for the final application. The theoretical criteria of the research, components of the experimental system, and key findings are presented in this report.

15. SUBJECT TERMS

Lidar; Oxygen; Raman spectroscopy; Remote sensing

16. SECURITY CLASSIFICATION OF:			17. LIMITATION OF ABSTRACT	18. NUMBER OF PAGES	19a. NAME OF RESPONSIBLE PERSON
a. REPORT	b. ABSTRACT	c. THIS PAGE			STI Help Desk (email: help@sti.nasa.gov)
					19b. TELEPHONE NUMBER *(Include area code)*
U	U	U	UU	24	(443) 757-5802